Three-Point Bending Crack Propagation Analysis of Beam Subjected to Eccentric Impact Loading by X-FEM

Toru Tsuda[1], Yoshihiro Ohnishi[2], Ryo Ohtagaki[1], Kyuchun Cho[3], Takehiro Fujimoto[3]

[1] ITOCHU Techno-Solutions Corp., Umeda, Kita-ku, Osaka, Japan
[2] ITOCHU Techno-Solutions Corp., Kasumigaseki, Chiyoda-ku, Tokyo, Japan
[3] Kobe University, FukaeMinami-machi, Higashinada-ku, Kobe, Japan

1 Introduction

When analyzing a failure or crack propagation problem by FEM, there are the following challenges to solve. (1)It's necessary to make element boundary match to the failure surface or the crack surface. (2)The failure shape and the crack propagation direction depend on the mesh. (3)It's necessary to express a singularity of crack tip field. (4)Both of the crack propagation path criterion and the crack propagation speed criterion are required. To overcome these challenges, Nishioka, et al. developed the moving finite element method which repeats mesh subdivision with crack propagation and succeeded to analyze a dynamic crack propagation problem with a high accuracy [1].
On the other hand, erosion technique generally is used to express the failure in fracture analysis by general-purpose FEM cord including LS-DYNA. However, it is difficult to evaluate it exactly from point of view as shown above.
In contrast, the extended finite element method; X-FEM [2] is expected as technique to overcome the above problem to be able to express crack propagation by adding a function to express a discontinuity and singularity of the crack to the shape function of the finite element instead of expressing the crack explicitly.
Therefore, in this study, we applied FEM with eroding technique and X-FEM for three-points bending of crack propagation problems of the beam subjected to eccentric impact loading. Then, evaluated problems and the effectiveness of each technique through the comparison with the experiment result.

2 Impact experiment

2.1 Test conditions

Impact three-point bending test of a beam with a pre-crack as shown in Fig. 2.1 was carried out by Cho, et al. [3]. The material of specimen used in this test is FC200 (grey cast iron). Dimension of the specimen (Length × Height × Thickness) is 250×50×25 mm and the beam span is 200 mm, as shown in Fig. 2.1. The initial crack length is 25 mm, and it is inserted into the center of specimen using electric spark machining. In addition, the initial fatigue crack of approximately 1 mm is inserted to using the hydraulic fatigue tester.

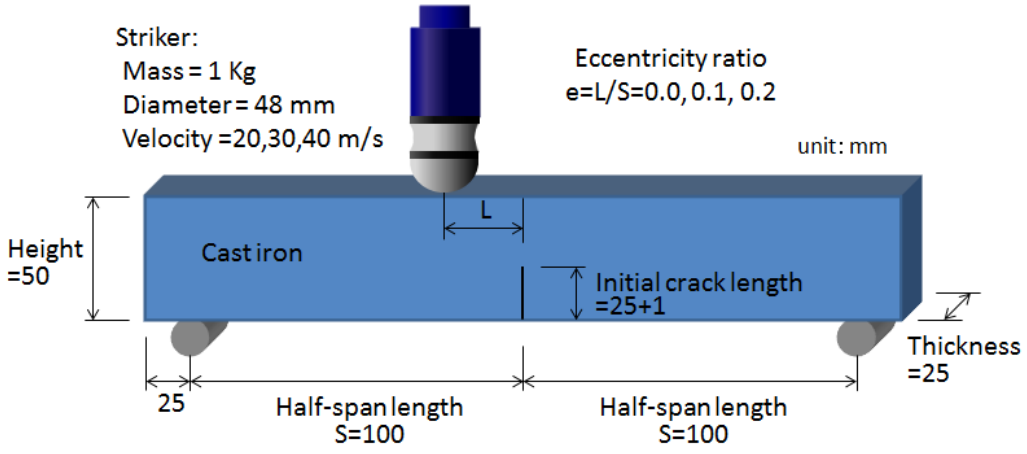

Fig. 2.1: Impact specimen

According to eccentric ratio [0.0, 0.1 and 0.2], the experiments carried out on shifted loading points from the specimen center. The high speed impact test was conducted under striker shooting velocity [20, 30 and 40m/s]. Table 2.1 indicates the test case.

Table 2.1: Test case

		Striker velocity (m/s)		
		20	**30**	**40**
Eccentricity ratio e=L/S	**0.0**	case11	-	-
	0.1	case21	case22	case23
	0.2	case31	case32	-

2.2 Test results

The crack propagation behaviors were observed by ultra-high-speed camera and a crack propagation movie was recorded to measure a crack velocity, fracture path and loading point displacement. The crack propagation images of each case as test result are show in Fig. 2.2.

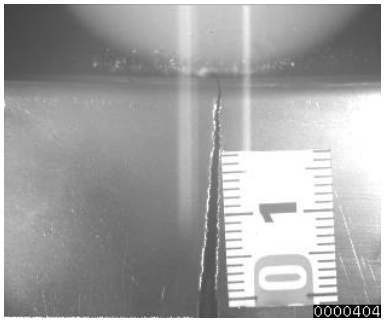

(a) case11

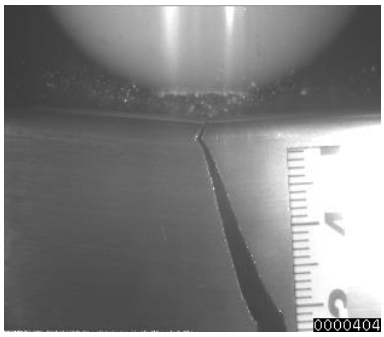

(b) *case21*

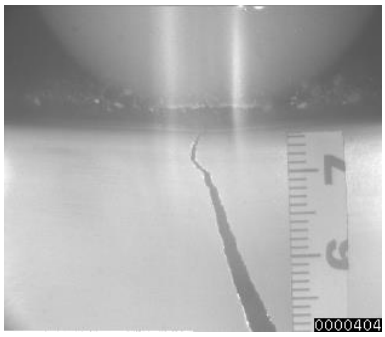

(c) case22

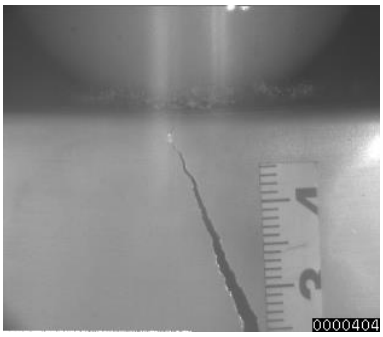

(d) case23

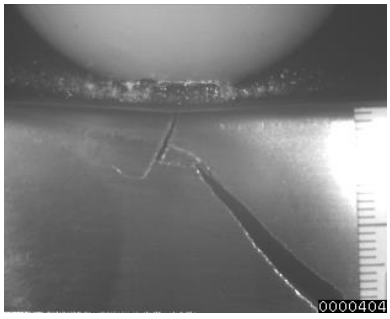

(e) case31

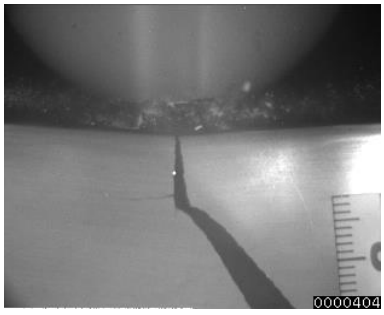

(f) case32

Fig. 2.2: Crack propagation images of each case

The fracture toughness was obtained as 39.306 $[\mathrm{MPa}\cdot\sqrt{m}]$ from these test results by Cho, et al. [3].

3 FEM analysis with eroding technique

In case of simulation for failure problem, the basic and easy method is to use standard FEM analysis with eroding technique. Therefore, before X-FEM analysis is carried out, we tried to use the basic method. The FEM mesh is shown in Fig. 3.1. The mesh size is 1 mm. In this section, only the case31 is carried out.

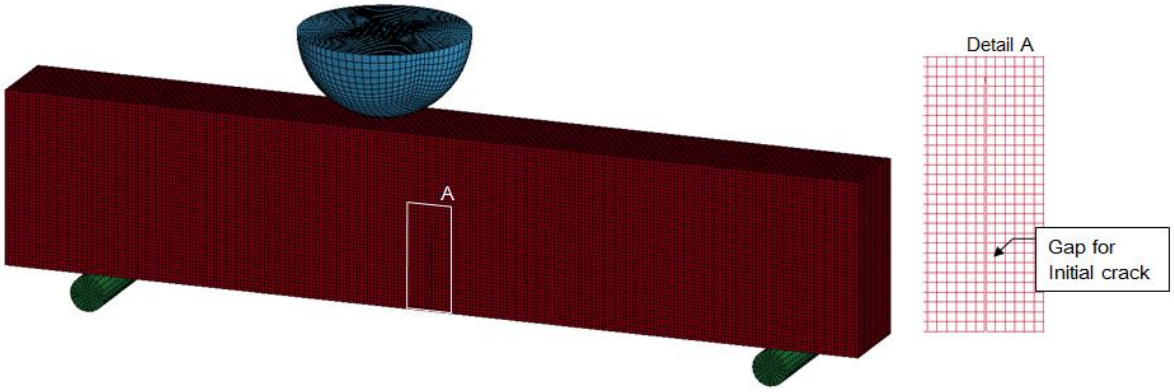

Fig. 3.1: mesh model

The material parameter is shown in Table 3.1. As criteria of element eroding, LS-DYNA has sevral parameters. One of most popular criterial for fracture analysis is maximum principle stress. Hence, at first, SIGP1 is used as eroding criteria in *MAT_ADD_EROSION.

Table 3.1: Material properties

Mechanical properties	value
Density [ton/mm^3]	7.04E-9
Young modulus [MPa]	100000
Poisson ratio	0.26
Maximum principle stress [MPa]	250

The crack propagation is shown at 0.038 [μsec], 0.061 [μsec], 0.07 [μsec], 0.10 [μsec] after impact in Fig. 3.2. Becase there are some element in thickness direction of cast iron, it is difficult to find all eroding area. Then, several element on surface is hidden.

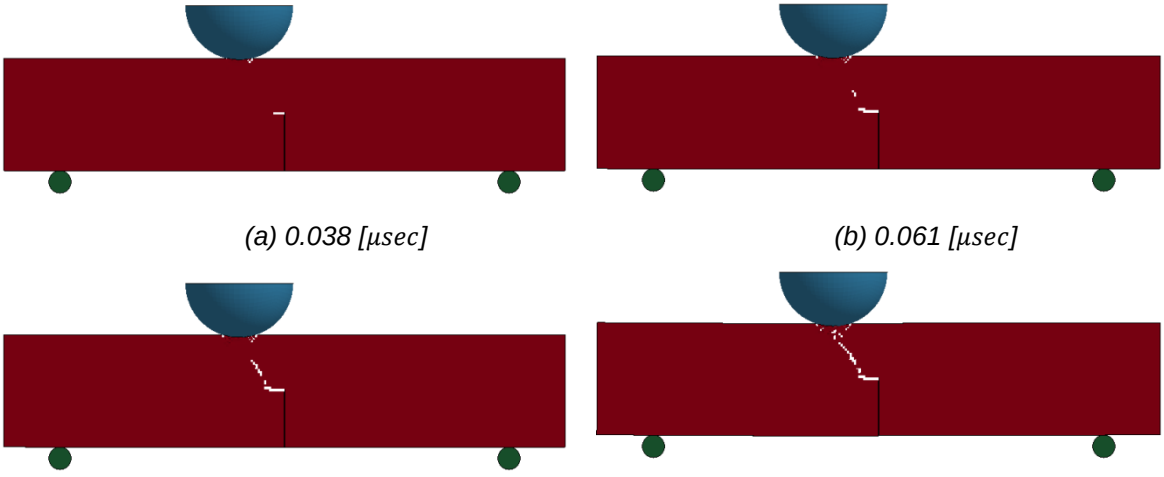

(a) 0.038 [μsec] *(b) 0.061 [μsec]*

(c) 0.07 [μsec] (d) 0.10 [μsec]

Fig. 3.2: Crack propagate

The crack propagated from edge of initial crack to striker point. It is not so far from experimental crack propagation. And there are some eroding element near contact area between striker and cast iron. In this area, it seems that there are too many eroding elements.
Normally, the tensile strength of FCD200 is over 200 [MPa]. But, it is measured by static tensile test. Thus, it may be higher in impact problem. Then, in case of higher eroding criteria, the result is shown in Fig. 3.3. The result of simulation has similar crack propagation and fewer eroding elements. Compare with test, the eroding situation in Fig. 3.3 is more similar than Fig. 3.2 near contact area. In addition to do it, the case of other failure criterial is carried out. One of them, the result using Pressure is shown in Fig. 3.4. In this result, there is no eroding area in near contact area.

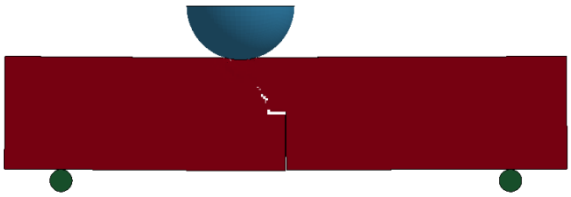

Fig. 3.3: Max principle stress 400 [MPa]

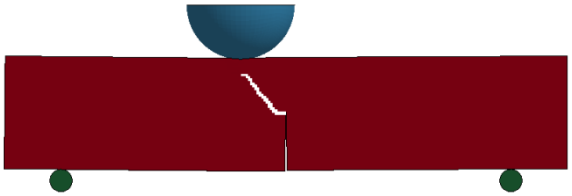

Fig. 3.4: Pressure 250 [MPa]

As above these results, this simulation is depend on which failure criteria is used and how much its value is. In addition to them, it is said that the normal finite element method with eroding technique is depending on mesh. Thereby, the case of finer mesh is carried out. The mesh size is half (0.5 mm). The simulation result is shown in Fig. 3.5. The failure criterion is max principle stress. Its value is 400 MPa.

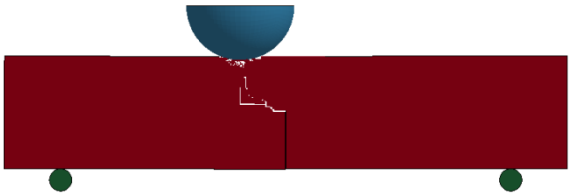

Fig. 3.5: Result on fine mesh

In this case, the eroding situation is different from the result on course mesh.
By using this method, we may be able to get good result. But, it is depend on failure criteria, its value and mesh. Thus, we should select better combination of them.

4 X-FEM analysis

4.1 Basic theory [4]

X-FEM has been implemented into LS-DYNA 971 for simulation of material failure and fracture analysis and currently, it is valid in two dimensional plane strain plates and shell structures. The cracks are represented by Level Set method and the kinetic relation governing the crack surface opening is simplified with cohesive material law.
In the X-FEM, the cracks are defined by the level set method as shown Fig. 4.1 (a). The surfaces of discontinuity Γ_α are described by a signed distance function

$$f(x) = \min_{\bar{x}\in\Gamma_\alpha} \|x-\bar{x}\| sign(n\cdot(x-\bar{x})) \quad (1)$$

$$g(x) = \min_{\bar{x}\in\Gamma'_\alpha} \|x-\bar{x}\| sign(n'\cdot(x-\bar{x})) \quad (2)$$

where $\bar{x}$ is a point on the surface of discontinuity Γ_α and n is a unit normal to the surface of discontinuity. The point $\bar{x}$ is the closest point to x and the orthogonal projection of x on Γ_α.
The discontinuity corresponds to $f(x) = 0$ and the two areas with different signs of $f(x)$ correspond to two domains across the discontinuity, as shown in Fig. 4.2 (b). The approximation close to the discontinuity (the shaded area in Fig. 4.2 (b)) consists of two parts. These are the standard finite

element approximation and the enrichment, as Eq. (3). Eq. (4) shows the enrichment of a Heaviside step function *H* for cracks cut through the element. Here, we ignored the term for crack tip singularity field $I \in C$. In the Eq. (3), Φ_I^{FEM} is a conventional finite element shape function and u_I and q_I are the regular and enriched nodal variables, respectively.

$$u^h(x) = \sum_{I=1}^{4} \Phi_I^{FEM} \cdot u_I + \sum_{I \in J} \Psi_I(x) \cdot q_I \tag{3}$$

$$\Psi_I(x) = \Phi_I^{FEM} \left\{ H(f(x)) - H(f(x_I)) \right\} \tag{4}$$

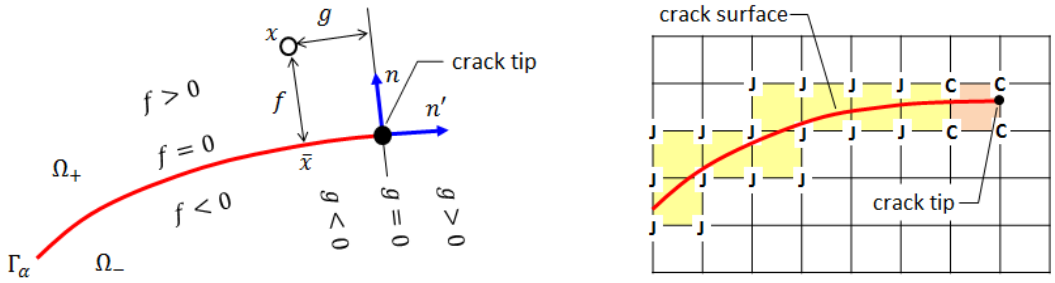

(a) Sign distance function *(b) Enriched element*

Fig. 4.1: X-FEM element defined by level set

4.2 General model setting of X-FEM [5]

Currently, two element types are available to be used in fracture analysis in LS-DYNA 971. For two dimensional plane strain plates, X-FEM element type 52 is based on 2D plane element type 13. For general shell structure, X-FEM element type 54 based on shell element type 16 can be used. The X-FEM element type is input in the keyword *SECTION_SHELL_XFEM.
The material type 185 (*MAT_COHESIVE_TH) is implemented to model the cohesive failure for the X-FEM element. This material model follows the cohesive law (Law I and Law II) with irreversible loading/unloading.
In order to define pre-cracks in a model, *BOUNDARY_PRECRACK card is used. Currently only simple pre-cracks can be defined, e.g., straight lines along one axis.
To record cracks in fracture simulation, one internal variable to the base element integration points. When the cohesive interface fails (it becomes a crack surface), this value will be one. In order to show the cracks in D3PLOT, one needs to use the keyword *DATABASE_EXTENT_BINARY to request LS-DYNA to store one additional history variable.
After calculation, LS-DYNA outputs two files (cracks and cracktip#). The cracks file contains the coordinates of the points that each crack surface intersects with element edges from starting crack point to ending crack point for all cracks. The cracktip# file shows the histories of crack tip locations for each individual crack #1, in the format “time, xc1, yc1, zc1, xc2, yc2, zc2”. We can confirm crack propagation histories by these two files.

4.3 Crack propagation criteria

The prediction of crack initiation/propagation-direction is governed by the maximum principal stress or the maximum shear stress. The other parameter, the critical crack opening displacement is computed from the critical energy release rate. When the maximum principal stress exceeds the critical value of each integration point in the near neighboring elements of the crack tip and the crack opening displacement reached the critical value, the crack propagate only one mesh, e.g. the crack tip jumps to other edge from an edge of the element and the element will be failed.

4.4 Cohesive material law [6]

The constitutive model used in the X-FEM is a cohesive model; material type 185. This cohesive material law is shown in Fig. 4.2.

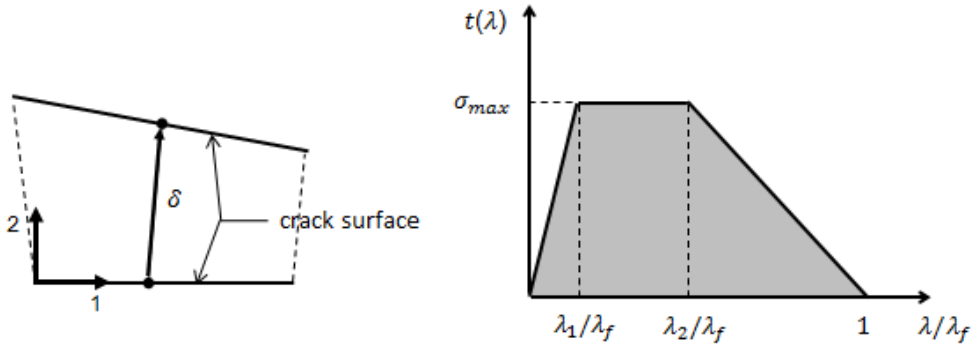

(a) Relative displacement *(b) Trilinear traction-separation law*

Fig. 4.2: Cohesive material law

In this cohesive material model, a dimensionless separation measure λ is used, which grasps for the interation between relative displacements in normal (δ_2-mode I) and tangential (δ_1-mode II) directions as shown in Fig. 4.2 (a):

$$\lambda = \sqrt{\left(\frac{\delta_1}{TLS}\right)^2 + \left(\frac{\langle \delta_2 \rangle}{NLS}\right)^2} \tag{5}$$

where the Mc-Cauley bracket is used to distinguish between tension ($\delta_2 \geq 0$) and compression ($\delta_2 < 0$). NLS and TLS are critical values, representing the maximum separations in the interface in normal and tangential direction.
For stress calculation, a trilinear traction-separation law as shown in Fig. 4.2 (b) is used. Moreover, tangential components (t_1) and normal component (t_2) of the tractionacting on the interface in the fracture process zone are given by:

$$\begin{bmatrix} t_1 \\ t_2 \end{bmatrix} = \frac{t(\lambda)}{\lambda} \begin{bmatrix} \frac{NLS}{TLS^2} & 0 \\ 0 & \frac{1}{NLS} \end{bmatrix} \begin{bmatrix} \delta_1 \\ \delta_2 \end{bmatrix} \tag{6}$$

4.5 Numerical analysis

We carried out impact three-point bending analysis by using X-FEM. The specimen as an elastic material (*MAT_001), is modeled with shell element (elform=2) and the striker and the fulcrum as a rigid body (*MAT_020), is modeled with solid element (elform=1) as shown in Fig. 4.3 (a). The yellow area in the figure is the range where X-FEM (elform=54) was applied with a cohesive law (*MAT_185). The mesh size of the specimen is 1mm and the shell thickness is 25mm.
The pre-crack is set by using *BOUNDARY_PRECRACK keyword as shown in Fig. 4.3 (b). Two dot points in the figure show the pre-crack points.

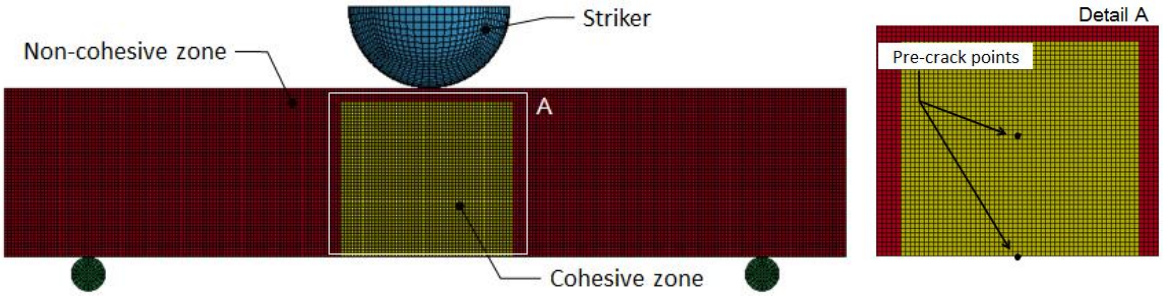

(a) 2D finite element mesh *(b) Position of initial crack*

Fig. 4.3: X-FEM analysis model

The material parameters of the specimen FC200 are shown in Table 4.1.

Table 4.1: Material properties

Mechanical properties	Value
Density ρ [ton/mm^3]	7.04E-9
Young modulus E [MPa]	100000
Poisson ratio ν	0.26
Fracture toughness K_{IC} [MPa · $\sqrt{m}$]	39.306

We converted to the energy release rate from the fracture toughness using the following equation and got 14.41 N/mm as the energy release rate G_{IC}.

$$G_{IC} = K_{IC}^{\ 2} \frac{(1-\nu^2)}{E} \tag{7}$$

Next, we investigated influence for crack propagation history about various analysis parameters and decided the suitable parameters as shown on Table 4.2, where SIGMAX is peak traction, NLS and TLS are length scale in the normal direction and length scale in the tangential direction, respectively. LAMDA1 and LAMDA2 are scale distance to peak traction and scale distance to beginning of softening, respectively. LAMDAF is scale distance for failure.
Here, SIGMAX was decided from the energy release rate and the crack tip opening displacement (CTOD), where it is know that the CTOD is small for Cast iron, which is brittle material. The critical value TLS for mode II was set similarly with NLS to consider a mix mode with load eccentricity. In addition, the extrinsic cohesive material law was used as shown in Fig. 4.4.

Table 4.2: Analysis parameters

Cohesive parameters	Value
SIGMAX [MPa]	1921
NLS, TLS [mm]	0.015
LAMDA1	0.0
LAMDA2	0.0
LAMDAF	1.0

X-FEM parameters	Value
ELFORM	54
BASELM	16
DOMINT	1
FAILCR	1

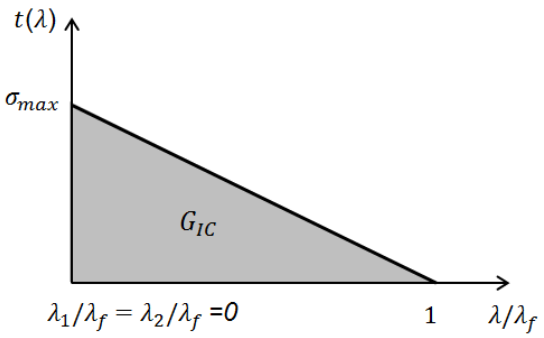

Fig. 4.4: Extrinsic cohesive law

4.6 Simulation results

Figure 4.5 shows the crack propagation histories of the test (left side) and the simulation (right side). Each test result was obtained from the image shown in Fig. 2.2 by Cho, et al. On the other hand, each simulation result is fringe component plot of “history var#1” in LS-PREPOST.

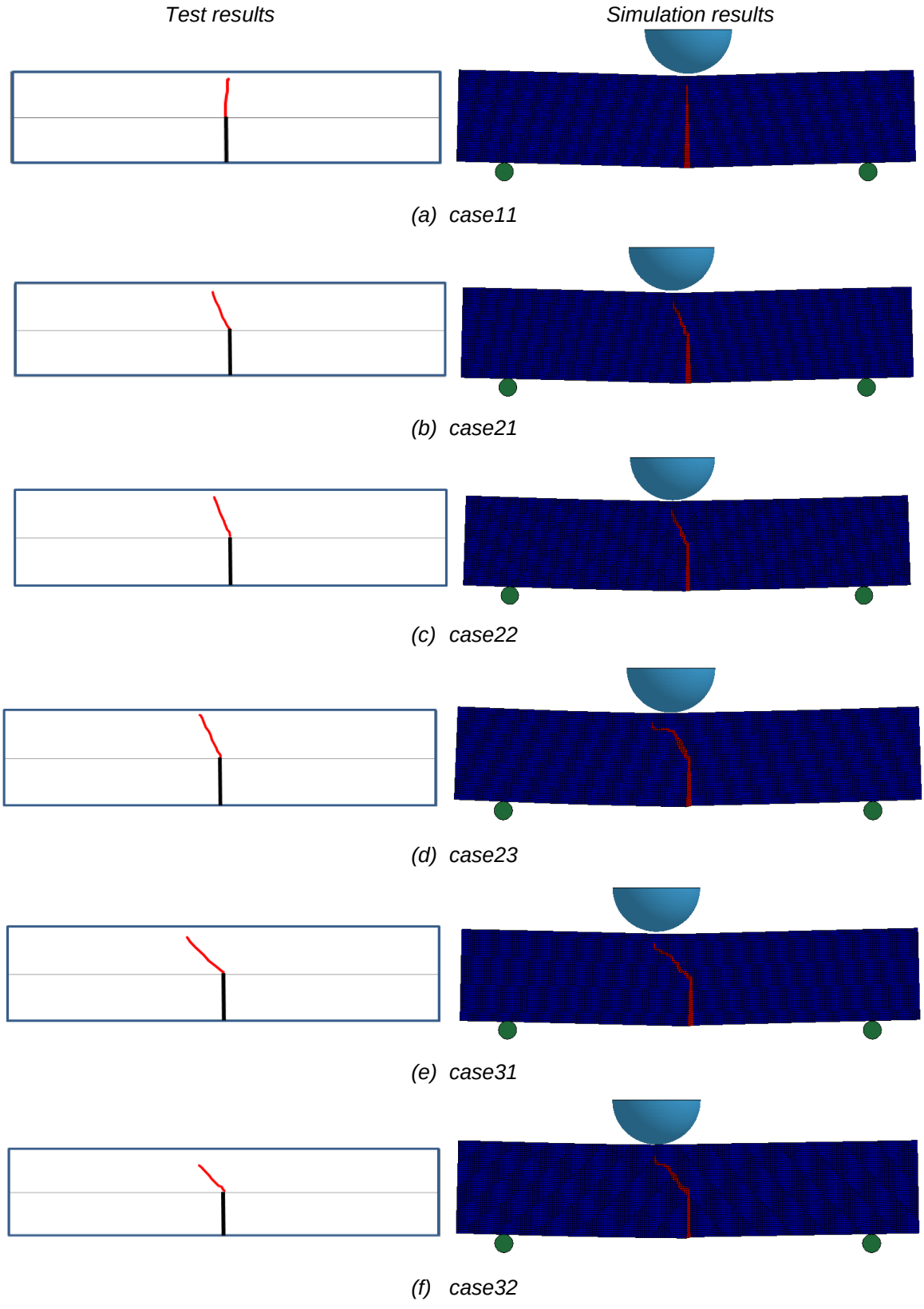

Fig. 4.5: Comparison of propagation path for each case

According to the figure, it is found that the simulation results are very similar to the test results in respect of the crack propagation path in each loading case.
Figure 4.6 indicates the crack propagation path in case21; this was obtained to plot the each crack tip coordinate of “cracks” file. The dot in the figure represents the crack tip points. It is found that the crack tip jumped from an edge to other edge.

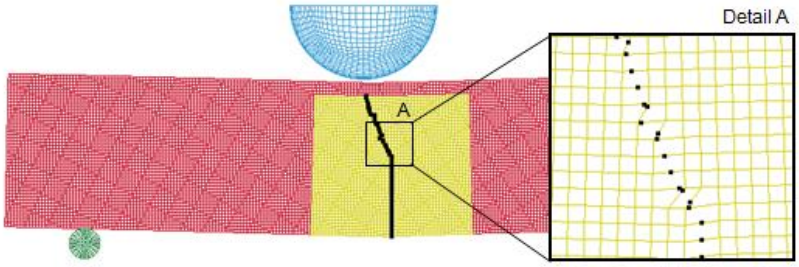

Fig. 4.6: Crack propagation path in case21

Finally, we checked the crack propagation criteria in case11. Figure 4.7 (b) shows maximum principal stress history of element of the crack front as shown Fig. 4.7 (b) at the crack initiation. The peak stress in the figure is about 1920 MPa. It is found that the stress decreased rapidly when the maximum principal stress exceeds SIGMAX and the element failed. When an element is totally failed, it means that the cohesive traction on the crack surface becomes zero and the crack surface becomes a free surface. However, the stress in the failed element as shown in the figure is not become zero because the integration points where the stress are calculated are not on crack surface.

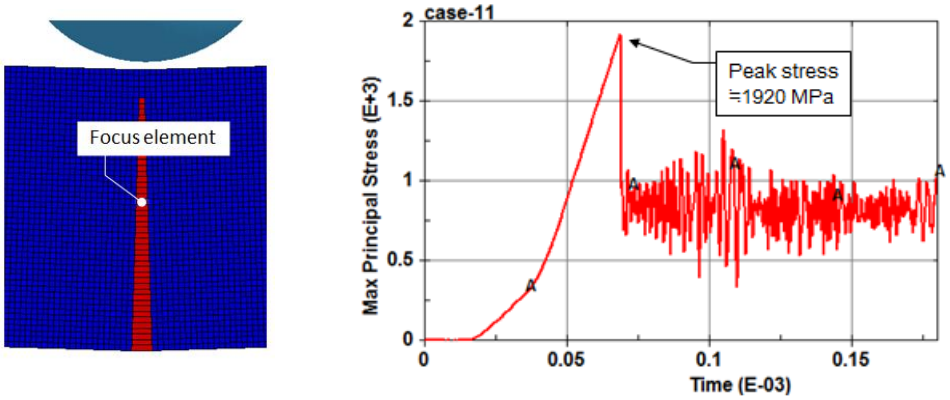

(a) Focus element of crack front *(b) Maximum principal stress history*

Fig. 4.7: The stress history of failed element in case11

5 Summary and discussion

In this paper, we tried to simulate three-point bending crack propagation of beam under the eccentric impact loading, and then the analysis results were compared with the experimental results. The simulation method we approached is the standard FEM with eroding technique and the X-FEM, which have been implemented in LS-DYNA.
As a result, the simulation roughly matched with the test. In particular, the crack propagation path obtained by the X-FEM agreed very well with the test, we could confirm that the X-FEM is very useful for crack propagation analysis. In addition, we investigated a basic function of X-FEM implemented into LS-DYNA. While the standard finite element method with eroding technique depends on mesh, it is an advantage that the X-FEM is independent of mesh.
On the other hand, there are several challenges as the followings in the X-FEM implemented into the current version of LS-DYNA. The X-FEM in LS-DYNA will be more practical if these capabilities are included into LS-DYNA.

(1) This function cannot apply to a 3D problem such as a torsion load, because a valid element type is limited to 2D element.
(2) Other new criteria for crack initiation and propagation are required as well as maximum principal stress criterion and maximum shear stress criterion.
(3) A new criteria to control crack propagation speed are required.
(4) A new mixed mode criteria using not only mode-I fracture toughness but also mode-II fracture toughness is required.
(5) A new method to express crack surface in LS-PREPOST is required.

6 Literature

[1] Nishioka, T., et al.:“Dynamic fracture-path prediction in impact fracture phenomena using moving finite element method based on Delaunay automatic mesh generation“, Int. J. Solids Struct., 38, 30-31, 2001, pp.5273-5301.
[2] Moes, N., Dolbow, J., Belytschko, T.:“A finite element method for crack growth without remeshing“, Int. J. Numer. Meth. Eng., 46(1), 1999, pp.131-150.
[3] Cho, K.C., et al.:“Experimental and numerical study on the dynamic fracture characteristics of grey cast iron FC200“, The 8th international symposium on impact engineering (ISIE2013), Sep., 2013.
[4] Guo, Y., Wu, C.T.:“XFEM and EFG Cohesive Fracture Analysis for Brittle and Semi-Brittle Materials“, The 11th international LS-DYNA users conference, 2010.
[5] “XFEM User’s Manual for LS-DYNA971“, LSTC, November, 2009.
[6] “LS-DYNA KEYWORD USER’S MANUAL VOLUME II“, LSTC, Janiary, 2013.